DOI: https://doi.org/10.46296/ig.v9i17.0321

EMULACIÓN DE UN SISTEMA HÍBRIDO DE MICROGENERACIÓN CON ALMACENAMIENTO E INYECCIÓN A RED

EMULATION OF A HYBRID MICRO-GENERATION WITH STORAGE SYSTEM AND GRID INJECTION

Guamani Ronny Santiago [1]; Quinatoa-Caiza Carlos [1]; Vaca Jimmy Roberto [2]

[1] University Technical of Cotopaxi, Department of Electrical Engineering. Latacunga, Ecuador. Correo: carlos.quinatoa7864@utc.edu.ec.

[2] Japan University Institute, Department of Electrical Engineering. Santo Domingo, Ecuador.

Resumen

Esta investigación muestra la simulación de una microrred híbrida con generación distribuida, sistema de almacenamiento y suministro de energía a la red, utilizando Simulink como medio. El objetivo es demostrar la viabilidad de incorporar recursos renovables, como la energía solar fotovoltaica y las baterías, en un sistema de baterías para alimentar una carga de 100 kW y gestionar los excedentes de una red de 440 V - 200 kVA. En este contexto, se creó un modelo que fusiona un sistema fotovoltaico de 85,2 kW, una batería de 6 kW y un sistema de baterías de 10 kWh, conectados mediante convertidores CC/CC y CC/CA. La simulación considera condiciones de operación típicas, incluyendo una irradiación solar de 1000 W/m². Se examinan variables fundamentales de la electricidad, como el voltaje, la corriente y la potencia, además del flujo de hidrógeno y la eficiencia del sistema en diferentes situaciones. Además, los resultados obtenidos indican que, tras un breve período de transición, el sistema alcanza un estado estable con tensiones trifásicas promedio de 506,27 V, corrientes de 2,69 A y una potencia activa promedio de 1308,58 W. Estas circunstancias facilitan una operación confiable y técnicamente adecuada para suministrar energía a la red. La onda sinusoidal, la estabilidad de las variables y la adecuada gestión del almacenamiento corroboran la viabilidad del modelo sugerido como una respuesta energética sostenible y escalable.

Palabras clave: Microrred híbrida, Generación distribuida, Energía fotovoltaica, Pila de combustible, Almacenamiento de energía, Inyección a la red.

Abstract

This research shows the simulation of a hybrid microgrid with distributed generation, storage system and energy supply to the grid, using Simulink as a medium. The objective is to demonstrate the feasibility of incorporating renewable resources, such as solar photovoltaic energy and batteries, in a battery system, in order to feed a 100-kW load and manage surpluses to a 440 V - 200 kVA grid. In this context, a model was created that merges an 85.2 kW PV system, a 6-kW battery and a 10-kWh battery system, connected through DC/DC and DC/AC converters. The simulation takes into account typical operating conditions, including a solar irradiation of 1000 W/m2. Fundamental variables of electricity such as voltage, current and power are examined, in addition to hydrogen flow and system efficiency in different situations. Furthermore, the results obtained indicate that, after a short transition period, the system reaches a stable state with average three-phase voltages of 506.27 V, currents of 2.69 A and an average active power of 1308.58 W. These circumstances facilitate reliable and technically appropriate operation to supply power into the grid. The sine wave, the stability of the variables and the adequate storage management corroborate the feasibility of the suggested model as a sustainable and scalable energy response.

Keywords: Hybrid microgrid, Distributed generation, Photovoltaic energy, Fuel cell, Energy storage, Grid injection.

Información del manuscrito:
Fecha de recepción: 13 de octubre de 2025.
Fecha de aceptación: 18 de diciembre de 2025.
Fecha de publicación: 12 de enero de 2026.

1. Introduction

The main challenge facing the world today is to minimize dependence on fossil fuels, a problem that can be mitigated by supporting renewable energies. Clean energy sources are expected to replace fossil fuels, not only because they are ecologically friendly (less CO2), but also because these energies are not only renewable, but also inexhaustible [1]. It is vital to look for techniques that improve the efficiency of these clean energies, but it is also vital to maintain an adequate connection between the renewable generator and the main connection system. In recent years, the need for electricity for commercial and industrial loads in urban and rural areas has grown exponentially [2]. Electrical energy can be produced from a variety of environmentally friendly sources, such as solar photovoltaics, wind power and fuel cells. These energy sources can effectively meet the energy needs of residential and commercial communities when professionally designed and installed.

Currently, the global landscape is on the verge of undergoing significant transformations in electricity usage, which requires a comprehensive study of a hybrid microgeneration system with storage and grid interconnection capabilities to effectively meet these upcoming challenges [1]. Current research highlights the incorporation of a photovoltaic (PV) microinverter into a hybrid energy storage system (HESS), which fuses batteries and high-density capacitors. As a result, efficient energy management in the microgrid was simplified through the use of advanced control techniques, such as real-time impedance modification, which contributes to improved power flow management [3]. In addition, an alternative study proposes a prototype hydrogen-oriented hybrid microgrid that combines solar and wind energy with hydrogen storage, with the objective of maximizing electrical energy absorption and fostering self-reliance through adaptive maximizing electrical energy absorption and fostering self-reliance through adaptive control techniques [3]. In addition, a microgrid employing energy conservation and generation systems effectively reduces power variations and prolongs battery durability [4].

This study highlights the enormous potential of hybrid microgrid systems to increase energy security linked to the grid. In particular, it has been shown that the incorporation of batteries and ultracapacitors, linked to virtual impedance control, is an effective tactic to manage these components in hybrid microgrids [1]. Simulations performed with Simulink have demonstrated the effectiveness of these procedures and have highlighted the advantages of a hydrogen-based microgrid, which promotes high self-control in solar and wind energy conservation [5]. A microgrid prototype including solar photovoltaic panels, a power generator and a battery storage system has been implemented. In comparison, the simulation of hybrid wind and photovoltaic microgrids in the PSCAD/EMTDC program includes a battery management strategy aimed at promoting autonomy and synchronized interaction with the grid. In the grid-tied application, the battery system regulates voltage levels and decreases power variations, while in stand-alone operation, the microgrid is quickly disconnected through a battery via P/V and Q/F adjustment mechanisms [6]. The evolution of hybrid microgrids faces the challenge of effectively merging renewable energy sources, such as solar and wind, together with conservation systems, thus ensuring balance and efficiency in the face of variations. It is crucial to develop sophisticated control algorithms to optimize energy management and extend the durability of the components. Despite the advances in simulation with Simulink [7], obstacles persist for the effective implementation of these technologies. This project seeks to solve these challenges through the development of simulation models and optimization algorithms, with the objective of increasing the safety and efficiency of hybrid microgrids in various operating situations [8]. Simulink, a pioneer in complex system modeling and transient configuration analysis, can effectively simulate a hybrid system that includes grid connectivity, solar power, fuel cells (FC), and BESS [9]. Figure 1 describes the fundamental design of a Hybrid Power Generation System along with its fundamental elements.

Fig. 1. *Fundamental design of a hybrid generation system.*

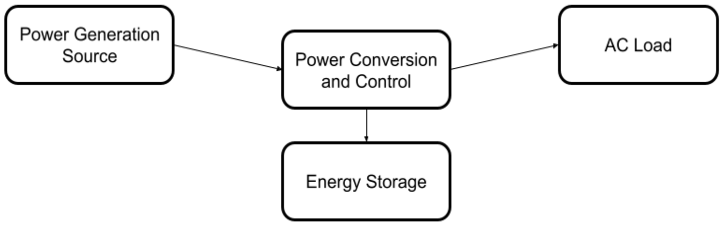

In remote areas, it is vital to guarantee a power supply. This involves linking the solar power array. This scheme promotes maximum utilization to increase the efficiency of solar energy conversion and energy transfer between the solar energy source and the main system [7]. A sophisticated framework of optimization mathematical algorithms has been developed for the operational monitoring of a hybrid energy complex, where a hydrogen generator is employed as a viable energy alternative. The efficiency of the system have been confirmed by extensive calculations [10], which facilitated the efficient simulation of a microgrid incorporating grid connections, fuel, solar photovoltaic (PV) systems and batteries, using sophisticated simulation software such as Simulink [11]. The microgrid simulation framework provides a comprehensive basis for evaluating various energy sources and loads over a 24-hour period of operation [12], which is crucial for understanding dynamic operations. In this scenario [13], a microgrid testbed can be set up to group these power sources and ensure stable operation in case of failure or disturbance, applicable in both grid-connected and stand-alone operation modes [14]. To optimize the performance of microgrids, various control tactics and algorithms are used, focusing particularly on battery management and power distribution. An energy management system (EMS) plays a crucial role in this optimization effort, since it structures energy resources and loads in a systematic way to enhance efficiency and economy [15].

A sophisticated particle swarm optimization algorithm was used to address optimization models linked to microgrid management, thus achieving effective integration of demand response strategies for load regulation. A framework for capacity configuration of photovoltaic (PV) systems, including energy storage and hydrogen solutions, was proposed and its validity was confirmed by case simulations and the study of optimization techniques [16]. An academic study using Simulink for analysis and simulation purposes focuses on energy management and performance evaluation, evidencing that the incorporation of battery storage significantly increases the operational efficiency of the solar photovoltaic (SPV) microgrid, generating remarkable power and fast response times, which favors the prolongation of the battery lifetime [17]. In addition, the integrated terminal sliding mode control (ITSMC) for switching voltage source inverter (VSI), tested in the Simulink framework [2], obtained a remarkable 97% efficiency in capturing solar energy for grid integration, effectively reducing the variations caused by high temperatures [18]. A simulation model designed in the Simulink environment incorporates a maximum power point tracking (MPPT) supervisor, whose objective is to guarantee the stability of the direct current (DC) microgrid [14]. This demonstrates that this framework protects any power source and thus maintains excellent stabilization under various load conditions; therefore, it is advisable to use sophisticated control methods for hybrid microgrids, favoring the assimilation of renewable energy along with storage [19].

2. Model of hybrid microgeneration system with storage system

The model presented as an example in Figure 2 is a basic emulation model of a micro-generation hybrid. This model integrates various energy sources, storage, and an electrical load, which simplifies the analysis of the operation of a complex energy system. Key elements include a fuel cell that generates energy through chemistry, a 25-kW photovoltaic that converts solar energy into direct current (DC), and a 10-kWh energy reservoir to ensure grid stability. The energy exchange between renewable energy sources, the storage system, and the central power system is made simpler by the interconnection of the components via DC/AC converters, transformers, and transmission lines [20].

Fig. 2. *The fundamental parts of a hybrid system.*

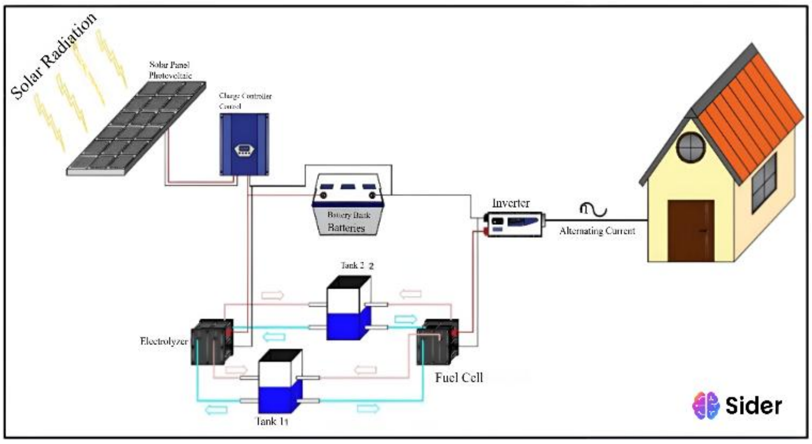

The model features a 200 kVA transformer that connects the microgrid to the larger grid, allowing the import or export of energy as needed. In addition, it has a 100-kW capacity that replicates the needs of an urban area. This simulation analyzes the management of energy flow in the microgrid. This process involves examining the dynamic reaction of the system to variations in energy production or consumption, and experimenting with control tactics, such as optimal energy emission. It also facilitates analysis of the efficient incorporation of renewable resources and on-line storage technologies [21].

Finally, the model incorporates sensors to measure essential variables such as voltages V_abc, currents I_abc and powers P_abc, which simplifies the system analysis. These calculations are essential for the elaboration and validation of control algorithms, guaranteeing stability in the operations and optimizing the energy performance of the microgrid. These simulations are useful tools for the creation of sustainable energy networks [22]. A general study of the essential elements is presented here in Table 1:

TABLE I. *FUNDAMENTAL ELEMENTS AND PARTICULARITIES OF MICROGENERATION*

Category	Component	Description
Generating Sources	Stack of Fuel Cells	Provides a hydrogen-based energy source
	Photovoltaic Array (PV Array 25 kW)	Converts solar energy into direct current (DC)
Energy Storage	10 kWh Battery	Stores energy to increase grid stability and withstand load variations

Energy Conversion	DC/DC Converters	Regulates the voltage and electricity produced by the renewable energy and storage system
	DC/AC Converter	Converts DC energy into AC for load application or grid administration
Charging and Grid Connection	100 kW Power Supply	Represents the use of the microgrid
	Interconnection with Power Grid (440 V, 200 kVA)	Facilitates energy supply to the grid in situations of overproduction

A. PEM Fuel Cell System Mode

To regulate the fuel storage voltage, it is crucial to consider the dynamism model. For some years now, researchers have developed PEM fuel storage devices, as shown in Figure 3. Therefore, the above models will be used [23].

***Fig. 3.** Design of a fuel cell.*

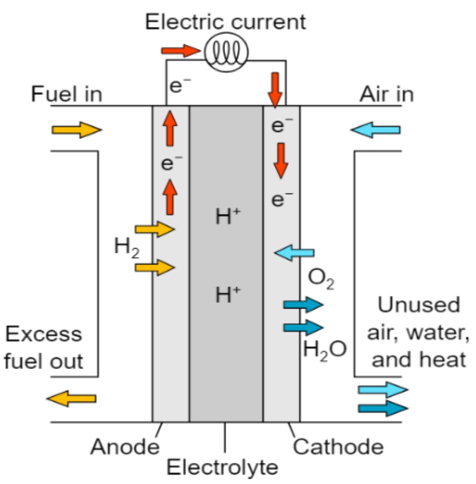

Equation 1 is used to determine the hydrogen production rate [11].

$$x_H = 5{,}18 * e^{-6} * I_e \quad (1)$$

Where x_H is measured in mole/s, while I_e refers to the current present at the ends of the electrodes.

To calculate the energy in hydrogen, equation 2 is used.

$$E_{H2} = \frac{Load}{\eta Fc} \quad (2)$$

Load symbolizes the maximum and minimum energy accumulation in kWh, while η_{FC} represents the fuel efficiency of the fuel to be loaded [11].

Next, the theoretical model of a PEM fuel cell for voltage, power and efficiency generation is presented.

Equation 3 can establish the stress produced.

$$U_s = U_{th} - U_{act} - U_{ohm} - U_{conc} \quad (3)$$

For this model, the theoretical U_{th} stress is determined from equation 4. It is necessary to consider the temperature variations in relation to the reference temperature [24].

$$U_{th} = 1{,}2297 + (T - 298{,}15)\frac{\Delta S_o}{nF} + \frac{RT}{nF} ln(\frac{P_{h_2} * P_{o_2 1/2}}{P_{o\,1/2}}) \quad (4)$$

Where *T* represents the operating temperature of the cell, ΔS_O refers to the entropy change of the liquid water application under standard situations of experiment with the value of -0.1634 KJ/k/mol, n represents the number of electrons per mole (n=2), *F* is the Faraday constant (96485.309 C/mol), and *R* is the general measure of the gas (8.31451 J/K/mol) [25].

With the calculation of the U_s voltage, it is possible to determine the power of the fuel cell using ohm's law (equation 5):

$$P_{pc} = I_{pc} * U_s \quad (5)$$

Where I_{pc} is set by the fuel cell manufacturer's specifications.

Equation 6 is used to calculate the fuel cell efficiency η_{pv}.

$$\eta_{stack} = 0{,}83 * \frac{U_s}{U_{th}} \quad (6)$$

B. Photovoltaic Solar Panel System

Solar panels are composed of modules and each module includes cells. It is essential to apply equation 7 for the dynamic current output [26].

$$I = N_p * I_{ph} - N_p * I_o * \left[exp\left(\frac{\frac{U}{N_S} + I * \frac{R_S}{N_P}}{n * V_t}\right) - 1\right] - I_{sh} \quad (7)$$

N_p refers to the number of parallel cells and N_s to the number of cells in series, U represents the voltage of each cell. To determine the power source I_{ph}, equation 8 is required to be applied [27].

$$I_{ph} = [I_{sh} + K_i(T - 298)] * \frac{I_r}{1000} \quad (8)$$

I_{sc} symbolizes the cut-off current (A), K_i describes the cell cut-off current at 25 °C at a solar irradiation of 1000 W/m2, T refers to the operating temperature in Kelvin (K) and I_r refers to the solar irradiation in W/m2.

To calculate the efficiency of the solar PV system, it is essential to know the input power Q_{in}, for which equation 9 is used [4].

$$Q_{in} = I_r * S_p * \alpha_{abs} \quad (9)$$

I_r represents the solar irradiance in W/m², S_p represents the surface area of the solar PV panel and α_{abs} is the global absorption coefficient [29].

By obtaining the two powers Q_{in} and P_{pv}, efficiency can be established using equation 10.

$$\eta_{pv} = \frac{Q_{in}}{P_{pv}} \quad (10)$$

C. Battery Power Supply and Disconnecting System.

The batteries are intended to store the surplus energy circulating through the voltage controller, in addition to saving, they are responsible for maintaining the voltage in the determined range and, consequently, safeguard the discharge rates and prevent overloading [30].

During the charging period, the relationship between voltage and current is exemplified by equation 11.

$$V = V_r + \frac{I\left(\frac{0{,}189}{1{,}142 - soc + R_i}\right)}{AH} + (soc - 0{,}9)ln\left(300\frac{I}{AH} + 1\right) \quad (11)$$

Where V_r is set by equation 12.

$$V_r = 2{,}94\,(1{,}0 - 0{,}001\,(T - 25°C\,)) \quad (12)$$

D. System Inverter

The properties are defined by the power entering the inverter and the power extracted from it. Inverters always suffer losses during conversion, so it is necessary to consider the manufacturer's data [11].

To calculate such output inverter power, equation 13 is used.

$$P_{inv-ip}\,\eta_{inv} = P_{inv-op} \quad (13)$$

E. Efficiency of the Hybrid System

Finally, to obtain the energy conversion efficiency of the solar panel system as a fuel cell system, equation 14 is applied [26].

$$\eta_{sh} = (P_{pv} + P_{pc})/(I_r * S_p) \quad (14)$$

In addition, the global flow of each numerical iteration of the microgeneration model is presented, which is represented from equation 1 to equation 14.

It begins with the introduction of the parameters required for the calculation of the microgeneration model. After the introduction of these parameters, each of the equations mentioned above is solved.

From equation 1 to 6, the fuel cell power includes the energy conversion process to determine the mass of hydrogen, energy storage. Equations 7 to 10 allow us to obtain the power output of the solar PV panel system, Equations 11 and 12 provide us with the charging and discharging voltage of the system batteries, Equation 13 helps us to obtain the AC current for our system, and finally, Equation 14 determines the efficiency of the hybrid system.

3. Validation of the hybrid microgeneration system with storage system

A. PV Array Data

Table 2 shows the key parameters of the 85.2 kW PV system during the simulation of a hybrid microgeneration. It incorporates 300 parallel strings, open circuit voltage (36.3 V), short circuit current (7.84 A) and operating parameters at maximum power, fundamental to assessing its performance.

TABLE II. *PV ARRAY CHARACTERISTICS*

Parameter	Value
PV array full power (kW)	85.2
Open circuit voltage Voc (V)	36.3
Short circuit current Isc (A)	7.84
Maximum power point voltage Vmp (V)	29
Maximum power point current Imp (A)	7.35
Parallel strings	300

B. Fuel Cell Data

The fuel cell has a maximum power of 8325 W and a nominal power of 5998.5 W, operating with high efficiency due to its low internal resistance and a Nernst voltage of 1.1288 V. It employs hydrogen and oxygen with efficiencies of 99.56 % and 59.3 %, respectively.

The system sustains constant fuel and air consumption, with an operating temperature of 338 K. Its design facilitates a broad spectrum of air and fuel flow, which is essential for variable applications. These properties make it perfect for high-efficiency hybrid power systems, as shown in Table 3 [25].

TABLE III. *FUEL CELL CHARACTERISTICS*

Parameter	Value	Unit
Stack power rating	5998.5	W
Maximum stack power	8325	W
Internal resistance	0.07833	Ω
Nernst voltage per cell	1.1288	V
Nominal utilization H_2	99.56	%
Nominal utilization O_2	59.3	%
Nominal fuel consumption	60.38	slpm
Nominal air consumption	143.7	slpm
Exchange current (i_0)	0.29197	A
Exchange ratio (α)	0.60645	—
Composition H_2	99.95	%
Composition O_2	21	%
Nominal fuel flow	50.06	lpm
Maximum fuel flow	84.5	lpm
Nominal air flow	300	lpm
Maximum air flow	506.4	lpm
System	338	K

temperature		
Fuel pressure (P_{fuel})	1.5	bar
Presión del aire (P_{air})	1	bar

C. Battery Data

Table 4 summarizes the most relevant parameters configured in the battery model in Simulink. The nominal voltage is 48 V, suitable for energy storage systems in residential or industrial applications. A high nominal capacity of 2100 Ah indicates a high autonomy.

The initial state of charge of 95% suggests that the battery starts almost fully charged. The rated discharge current of more than 900 A reflects its ability to supply under demanding conditions. Finally, the extremely low internal resistance ensures high efficiency in energy delivery, minimizing heat losses.

TABLE IV. *BATTERY DATA*

Parameter	Value	Unit
Nominal voltage	48	V
Nominal capacity	2100	Ah
Initial state of charge	95	%
Rated discharge current	913.04	A
Internal resistance	0.00022857	Ohm

D. Modeling of the Simulation

Figure 4 presents the fundamental elements of a hybrid microgeneration system with storage system. This schematic shows the connection of each of the components, starting from the solar PV panel, which is linked to a charge controller. The charge controller plays an essential role in the energy management of the system. One of its primary tasks is to protect the battery bank from overcharging, ensuring that its output voltage remains within a safe range. If the voltage exceeds the allowable limit, the controller will disconnect the load to prevent damage to the system.

Fig. 4. *Simulink is a general model of microgrid.*

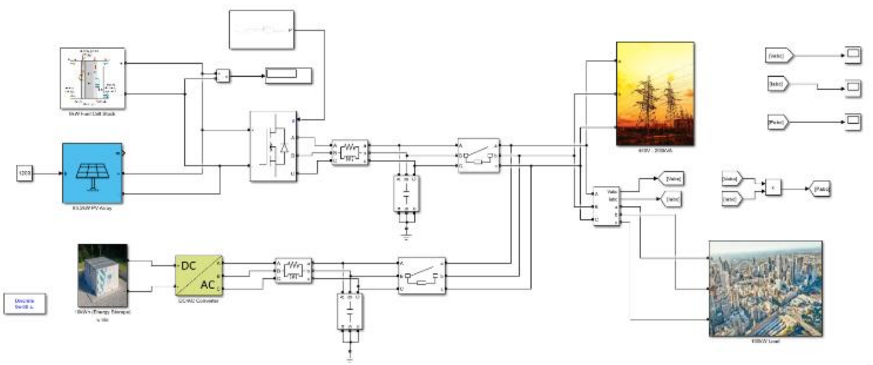

In addition, the charge controller controls the current to the battery. If the solar panel provides excessively low current, the system will also disconnect the load until conditions are re-established. When the voltage and current return to appropriate levels, the controller will re-enable the system connection, ensuring efficient and safe operation [31].

The Simulink simulation shows that the system is made up of a DC/AC converter, a 6-kW battery, and a 10-kWh battery bank. It is necessary to verify how these elements relate to one another and make certain adjustments in order to adapt the simulation to the given text. The batteries need to be linked to the electrolyzer, allowing them to supply power until they reach their discharge limit. This will ensure that the electrolysis system operates constantly, producing hydrogen to supply fuel to the cell. Both the battery and the fuel container operate on direct current (DC), which is in accordance with the system specification. To achieve an alternating current (AC) output with a nominal voltage of 120 V, the system requires the presence of an inverter.

In the simulation, a DC/AC converter is already present, whose function is to convert the energy obtained from the batteries and the fuel tank into alternating current. It is crucial to ensure that the configuration of this inverter enables 120 V output, so that the power can be used in a household.

If the simulation still does not show this process accurately, it would be imperative to add an electrolyzer block that receives power from the battery and fuel storage. In addition, it is necessary to ensure that the inverter operates properly to produce the 120 V AC output.

E. Applied Methodology of the Microgrid

In Figure 5, the energy source data is entered, which includes the PV system, fuel storage, battery, grid and load. Then, the generation is modeled using the solar panels and the fuel cell [16].

Fig. 5. Methodology Applied in the Simulation.

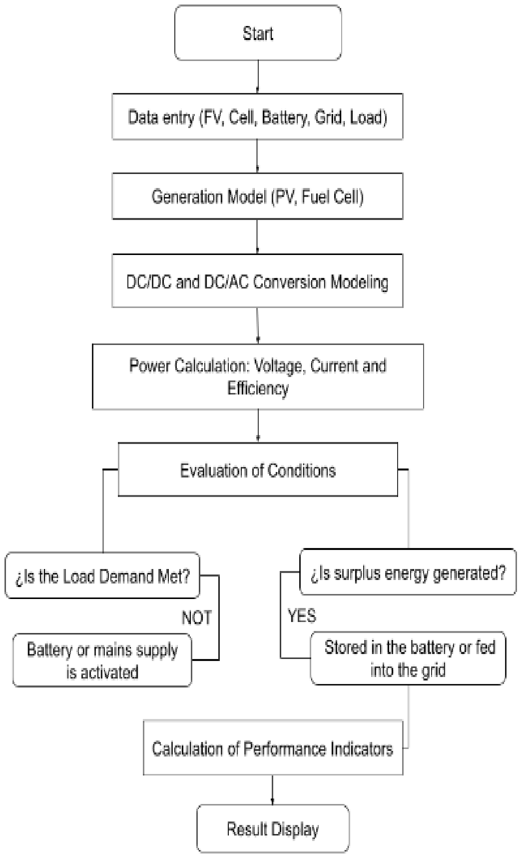

Then, energy transformation is performed through the DC/DC and DC/AC converters to achieve the required energy type. With this data, the power calculation is performed taking into account voltage, current and efficiency.

The evaluation of the system conditions is then carried out. If the load requirement is not met, the battery or the supply from the grid is started. If surplus energy is produced, it is stored in battery storage or supplied to the grid. Finally, the performance indices are determined and the results achieved are displayed.

4. Results of the microgeneration system

This section presents the study of the graphs generated through simulation in the Simulink program, linked to the emulation model of a hybrid microgeneration with storage system and grid injection. The system consists of an 85.2 kW photovoltaic system, a 6-kW fuel source and a 10-kWh storage system. All these elements operate synchronously to ensure the supply of electricity to a 100-kW load and the management of surplus to the 440 V - 200 kVA grid.

A study of the system's behavior under normal operating conditions is carried out, taking into account irradiance levels of 1000 W/m2. In this research, voltage, current and power parameters are analyzed in the different stages of energy transformation, in addition to the effect of solar radiation variability on the system performance. It is assumed that the fuel cell functions as a backup in case the primary generation is insufficient.

Additionally, the behavior of the hydrogen flow in the fuel cell and the efficiency of the energy storage are analyzed. A crucial element of the research is the assessment of the data based on domestic loads, without considering special loads. For a better understanding of the findings, tables with the technical characteristics of the equipment used in the study will be provided.

A. Voltage at Load

The simulation depicts, in Figure 6, the change of the three-phase voltage as time elapses in the hybrid microgrid. The time is shown on the horizontal axis, with a scale from 0 to 0.5 seconds, while the voltage is shown on the vertical axis, which oscillates approximately between -800 V and 800 V.

In the first 0.05 seconds, the signal shows a transient behavior with oscillations of large amplitude, reaching peaks exceeding 700 V. This indicates that, during system start-up or during source synchronization, the voltage may vary before the system achieves stability.

After 0.1 seconds, the oscillations start to decrease, and a more consistent sinusoidal signal is perceived. This behavior suggests that the microgrid has managed to remain in a steady state, with maximum and minimum values close to ± 600 V, which could be equivalent to a system with an effective voltage of about 440 V. This behavior signals that the microgrid has managed to synchronize with the distribution grid and that the DC/AC conversion of the inverters is working properly.

It is vital to emphasize that the quality of the voltage at the first transient can affect system stability and cause grid disturbances. To mitigate this effect, more robust control tactics in inverters and energy storage could be examined.

__Fig. 6.__ Microgrid on-load voltage

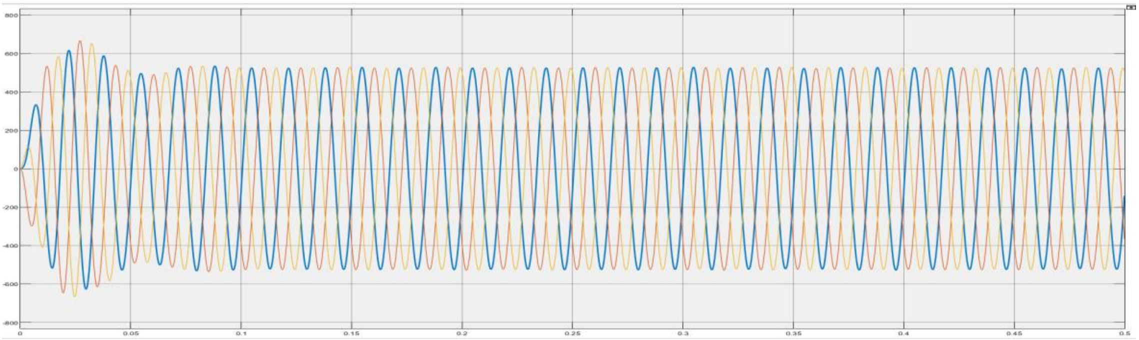

B. Current Intensity in the Load

The simulation in Figure 7 shows the behavior of the voltage and current signals as time passes, which facilitates the analysis of the stability and quality of power in the microgrid.

The time is located on the horizontal axis and fluctuates between 0 and 0.5 seconds. In the first 0.05 seconds, a transient stage is perceived, characterized by large amplitude oscillations in both voltage and voltage. This behavior is typical of systems where there is a synchronization process between the energy sources and the grid, as in the connection of inverters or in the supply of energy from the storage system.

With respect to the current, initial variations can be observed that later consolidate into a sine wave with stable frequency, signaling that the system has reached a steady state after startup. Although the current follows the pattern of the voltage, it is crucial to examine the relationship between the two to establish whether there are phase shifts, harmonics or other events that may influence the efficiency of power injection into the grid.

In the steady state (after 0.1 second), both current and voltage exhibit periodic oscillation, indicating that the inverter control system is operating properly to control the power conversion. To enhance the stability and quality of the power supplied to the grid, sophisticated control tactics, such as the implementation of predictive controllers or active filters, could be applied to help reduce harmonics and optimize synchronization with the grid.

C. Power in the Load

The simulation in Figure 8 describes the progression of the current overtime in a microgeneration system. It is possible to distinguish two fundamental phases in the behavior of the current: an initial transient stage and a subsequent stationary stage.

During the transient phase, which occurs around 0 to 0.1 seconds, an accelerated increase in current is noted. During the first 0.05 seconds, there is a peak that reaches figures close to 2500 units (probably in amperes or milliamps, depending on the scale used in the simulation).

Then, the current oscillates with a slight decrease in amplitude, indicating that the system is adapting to the new operating situation. This momentary behavior is distinctive when a generation source starts supplying electricity to the grid or when there is a drastic variation in demand.

From 0.1 seconds, the system enters a steady state where the current stabilizes in a frequency-invariant sine wave. The range is sustained at around 1000 to 1500 units, indicating that the system has achieved a stable operating regime. The waveform has a regular shape and appears to be properly synchronized, indicating that the inverter control and storage strategy are operating properly.

However, there are some observations and possible improvements that could be implemented. First, the control system could be refined to minimize the initial peak current, since high values can cause stress on the electrical elements.

Fig. 7. *Current intensity in the load in the microgrid.*

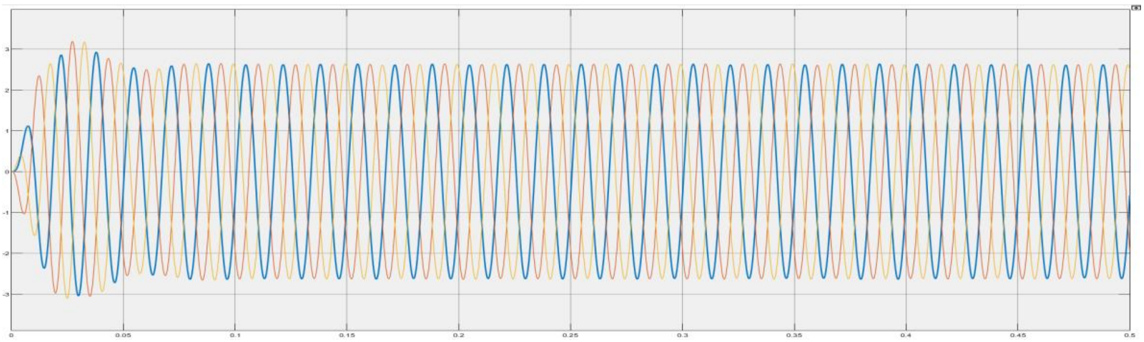

Additionally, it would be advisable to carry out a study of the signal quality to confirm the existence of harmonics that could influence the efficiency of power management.

Finally, if the system has an inverter, modifying its regulation could help to smooth the synchronization process with the grid and minimize possible oscillations in the transient regime.

With the results achieved, it is technically feasible to supply power to the grid. The average active power of 1308.58 W, although low, is a valuable contribution in the framework of distributed generation, particularly in residential or small-scale commercial uses. The average three-phase voltage of 506.27 V and current of 2.69 A indicate operation suitable for the low-voltage grid.

Fig. 8. *Power in the microgrid load.*

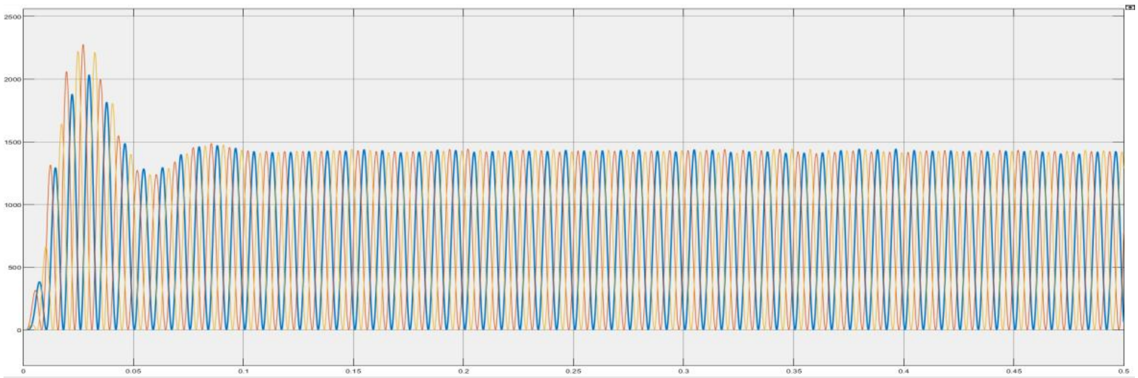

5. Discussion

The dynamics of the system in relation to three-phase voltage, current and power are shown below.

- Figure 6 shows the temporal development of the three-phase voltage at the inverter output. In the first milliseconds (about 0 to 0.05 seconds), a transient state, common during system startup, is manifested. After that time, the voltage stabilizes to a symmetrical sinusoidal signal with an effective amplitude reaching 500 V, demonstrating proper synchronization with the power grid.
- Figure 7 shows the three-phase current that has been injected. Similarly to the voltage, the current undergoes a small initial oscillation before reaching a steady state. Once the transient has been overcome, the waveform remains sinusoidal

and phase-balanced, with an average amplitude close to ±3 A, signaling stable and efficient operation of the system in terms of current delivery.

- Finally, graph 8 shows the progress of the three-phase power provided. At the beginning, a start peak is perceived around 2000 W, product of the coupling of the production sources (solar photovoltaic, fuel cell and battery). Then, the power remains stable at a constant average value close to 1300 W, which demonstrates the ability of the system to ensure a constant power supply to the grid.

To measure the behavior of the system for each of the key variables, the following table 5 was created. It lists the highest, lowest and a stable average (calculated as the average of the most recent simulated data) for three-phase voltage (V), current (A) and power (W).

With the results achieved, it is technically feasible to supply power to the grid. The average active power of 1308.58 W, although low, is a valuable contribution in the framework of distributed generation, particularly in residential or small-scale commercial uses. The average three-phase voltage of 506.27 V and current of 2.69 A indicate operation suitable for the low-voltage grid.

In addition, the balanced and sine waveforms demonstrate proper synchronization of the inverter with the grid, satisfying power quality standards. This ensures that the injection does not cause harmful disturbances or imbalances. Although the power quantity is restricted, its constancy and quality corroborate its feasibility. These types of systems, when multiplied on a large scale, can have a significant impact on the backup of the electrical grid, favoring the decentralization of the energy system and boosting operational efficiency.

TABLE V. *SYSTEM PERFORMANCE*

Variable	Maximum	Minimum	Steady State Average
Voltaje (V)	563.19 V	-561.00 V	506.27 V
Current (A)	3.01 A	-3.00 A	2.69 A
Power (W)	2000.21 W	-39.96 W	1308.58 W

6. Conclusions

The simulation performed shows that the suggested hybrid system is technically and operationally effective for the production and distribution of electrical energy. The model manages to effectively merge a photovoltaic source, a fuel tank and a storage system, ensuring stability in the fundamental variables: voltage, current and power. Stable operation, after a short transient period, corroborates the system's response to typical load situations. Additionally, the balanced and sinusoidal waveforms confirm the synchronization of the inverter with the grid. This suggests that the system is suitable for real distribution generation applications.

The findings from the graphs show that the quality of the power produced meets the criteria required for supply to the grid. The stable three-phase voltage around 506 V and the balanced currents around 2.7 A indicate that the system is free of distortions and unbalances. In addition, the inverter retains a suitable shape and frequency, ensuring compatibility with low-voltage grids. This ability to adapt transforms hybrid micro-generation into an effective answer to backing up the traditional power grid with clean and stable energy.

Although the simulated system provides an average power of 1308.58 W, its relevance lies in its ability to be scalable. This type of distributed generation, in residential or commercial situations, can reduce the need for centralized sources and minimize transmission losses. Additionally, the incorporation of storage enables greater energy independence and storage capacity. The system, replicated in several units, could contribute significantly to the electric grid, promoting a sustainable energy transition. Thus, the model constitutes a strong foundation for future applications of hybrid microgrids in urban or rural areas.

References

[1] P. Gaisse, J. Munoz, M. Rivera, C. Restrepo, and G. Mirzaeva, "Photovoltaic Microinverter with Hybrid Energy Storage System (HESS) and Virtual Impedance Control for Injection into a Microgrid," Nadi, Mar. 2022, pp. 1–7. doi: 10.1109/SPEC55080.2022.10058296.

[2] R. M. Meenakshi and K. Selvi, "Controller design for a Single-Stage Single-Phase Grid-Connected Solar PV Microgrid," *2023 Second International Conference on Electrical, Electronics, Information and Communication Technologies (ICEEICT)*, pp. 1–4, 2023, [Online]. Available: https://api.semanticscholar.org/CorpusID:259279749

[3] J. Villa Londono, A. Mazza, E. Pons, H. Lok, and E. Bompard, "Modelling and Control of a Grid-Connected RES-Hydrogen Hybrid Microgrid," *Energies (Basel)*, vol. 14, p. 1540, Mar. 2021, doi: 10.3390/en14061540.

[4] F. Remache, J. Castillo, C. Quinatoa, and L. Camacho, "Simulation of Hybrid PV Solar System with Fuel Cell in MATLAB Simulink," *WSEAS Transactions on Circuits and Systems*, vol. 23, pp. 172–183, 2024, doi: 10.37394/23201.2024.23.18.

[5] S. Chava, M. Kumar, V. Rajeswari, and S. Gowri, "Design of Hybrid Micro-grid under Islanding and Grid Connected Modes," Erode: IEEE, Mar. 2022, pp. 839–845. doi: 10.1109/ICSCDS53736.2022.9761024.

[6] A. Biswal and K. Roy, "Modelling and Performance Analysis of a Hybrid Wind and PV Generation System," Bhubaneswar, India: IEEE, Mar. 2022, pp. 1–6. doi: 10.1109/ODICON54453.2022.10009994.

[7] B. Harish and U. Surendra, "Power quality disturbance mitigation in grid connected photovoltaic distributed generation with plug-in hybrid electric vehicle," *International Journal of Electrical and Computer Engineering (IJECE)*, vol. 13, p. 6025, Mar. 2023, doi: 10.11591/ijece.v13i6.pp6025-6036.

[8] R. E. M. Vega, N. M. S. Herrera, O. R. Hernández, M. Robles, and J. R. R. Rodríguez, "Validación de una microrred mediante software in the loop para la inyección de potencia activa en redes eléctricas de distribución," *Ingeniería Investigación y Tecnología*, 2024, [Online]. Available: https://api.semanticscholar.org/CorpusID:273270506

[9] O. Krishan and S. Suhag, "Grid-independent PV system hybridization with fuel cell-battery/supercapacitor: Optimum sizing and comparative techno-economic analysis," *Sustainable Energy Technologies and Assessments*, vol. 37, p. 100625, 2020, doi:

https://doi.org/10.1016/j.seta.2019.100625.

[10] V. Ram, Infantraj, and S. R. Salkuti, "Modelling and Simulation of a Hydrogen-Based Hybrid Energy Storage System with a Switching Algorithm," *World Electric Vehicle Journal*, vol. 13, no. 10, pp. 1–88, Oct. 2022, doi: 10.3390/wevj13100188.

[11] P. A. Gbadega and A. K. Saha, "Impact of Incorporating Disturbance Prediction on the Performance of Energy Management Systems in Micro-Grid," *IEEE Access*, vol. 8, pp. 162855–162879, 2020, doi: 10.1109/ACCESS.2020.3021598.

[12] L. Stoyanov, "Modeling of Hybrid System with Photovoltaic Panels-Fuel cells Generation and Hydrogen Storage Using Electrolyzer," Sofia, Bulgaria, Mar. 2021, pp. 1–4. doi: 10.1109/ELMA52514.2021.9502964.

[13] V. Teterev and I. Khudiakov, "Simulation of a Hybrid Solar Power Plant with a Hydrogen Generator in MATLAB/Simulink Environment," *Lighting Engineering & Power Engineering*, vol. 61, pp. 30–48, Mar. 2022, doi: 10.33042/2079-424X.2022.61.2.01.

[14] J. Solano, D. A. Jimenez, and A. Ilinca, "A Modular Simulation Testbed for Energy Management in AC/DC Microgrids," *Energies (Basel)*, vol. 13, pp. 40–49, 2020, doi: https://doi.org/10.3390/en13164049.

[15] F. I. Masango, J. A. Jordaan, and A. F. Nnachi, "Modeling and Analysis of Residential DC Microgrid Energy Management Using System of Systems Architecture," *2023 IEEE AFRICON*, pp. 1–6, 2023, [Online]. Available: https://api.semanticscholar.org/CorpusID:264881687

[16] L. Camacho, S. Marrero, and C. Quinatoa, "Emulation of a PEM Fuel Cell Stack from its Generic and Polynomial Model using Simulink," *WSEAS TRANSACTIONS ON CIRCUITS AND SYSTEMS*, vol. 23, pp. 92–103, Mar. 2024, doi: 10.37394/23201.2024.23.9.

[17] Z. Xu, F. Chen, X. Yang, and Q. Lu, "Optimal Capacity Planning of a PV-Battery-Hydrogen System for Microgrid in Grid-Connected Mode," *J Phys Conf Ser*, vol. 2785, p. 12084, Mar. 2024, doi: 10.1088/1742-6596/2785/1/012084.

[18] A. Muntaser, H. K. Ragb, and I. Elwarfalli, "DC Microgrid based on Battery, Photovoltaic, and fuel Cells;

Design and Control," *ArXiv*, vol. 22, pp. 1–8, 2022, doi: https://doi.org/10.48550/arXiv.2212.14803.

[19] A. Narasimhan, "Simulation of Microgrid Technology by modelling Solar Plant and Battery System," in *2020 IEEE International Conference on Electronics, Computing and Communication Technologies (CONECCT)*, 2020, pp. 1–6. doi: 10.1109/CONECCT50063.2020.9198581.

[20] U. Manassero, A. S. Loyarte, and E. Salvetti, "Design and Evaluation of a Micro-Grid with Hybrid Diesel-Photovoltaic Generation and Storage in a Rural District," *2020 IEEE Congreso Bienal de Argentina (ARGENCON)*, pp. 1–8, 2020, [Online]. Available: https://api.semanticscholar.org/CorpusID:237001189

[21] H. R. H. Arhuata, J. C. Huaraya, V. S. Mamani, W. M. S. Vilcapaza, R. D. M. Apaza, and J. T. Yucra, "Proposal for the implementation of topologies in public lighting systems with micro-inverters and injection to the grid with photovoltaic solar energy," 2024. [Online]. Available: https://api.semanticscholar.org/CorpusID:269744470

[22] M. T. Vaïtchemé, S. H. Fouad, and S. Georges, "Modelling and performance analysis of a PV system with lithium-ion battery for autonomous micro-grids," in *2023 6th International Conference on Renewable Energy for Developing Countries (REDEC)*, 2023, pp. 30–35. doi: 10.1109/REDEC58286.2023.10208172.

[23] D.-C. Urcan, G. Fierăscu, D. Bică, L. Ioan Dulău, I. Vlasa, and M. Arhip-Călin, "Simulation and Monitoring of Energy Flows in a Micro-Grid," in *2020 55th International Universities Power Engineering Conference (UPEC)*, 2020, pp. 1–6. doi: 10.1109/UPEC49904.2020.9209828.

[24] P. Horrillo-Quintero *et al.*, "Dynamic Fuzzy Logic Energy Management System for a Multi-Energy Microgrid," *IEEE Access*, vol. 12, pp. 93221–93234, 2024, doi: 10.1109/ACCESS.2024.3422009.

[25] P. Di, Z. Su, Q. Lu, J. Liu, K. Xu, and G. Yan, "Optimal Energy Management for Multi-energy Microgrid Considering Demand Response," in *2022 IEEE 6th Conference on Energy Internet and Energy System Integration (EI2)*, 2022, pp. 72–77. doi: 10.1109/EI256261.2022.10117134.

[26] S. Jiang, L. Tang, Z. Shi, N. Shu, H. Huang, and F. Fan, "Coordinated Optimization Strategy for Topology Configuration of Wind-Solar-Hydrogen-Storage Multi-Energy Microgrid," in *2023 IEEE 7th Conference on Energy Internet and Energy System Integration (EI2)*, 2023, pp. 736–740. doi: 10.1109/EI259745.2023.10512590.

[27] H. Cai, Q. Guo, M. Su, S. Liu, W. Wu, and L. Huang, "Research on Hybrid Real-time Simulation Interface of RTDS Digital and Physical Model," in *2021 China International Conference on Electricity Distribution (CICED)*, 2021, pp. 1–7. doi: 10.1109/CICED50259.2021.9556823.

[28] S. Kumar and M. P. Selvan, "Modelling and Demonstration of Flywheel Energy Storage Sysetm for Micro-grid Applications," in *2023 11th National Power Electronics Conference (NPEC)*, 2023, pp. 1–6. doi: 10.1109/NPEC57805.2023.10384898.

[29] L. D. R. Dueñas and J. L. S. Saquicela, "Simulación de la operación de redes de energía inteligentes mediante modelos de demanda de potencia usando Matlab," *Brazilian Applied Science Review*, 2022, [Online]. Available: https://api.semanticscholar.org/CorpusID:252673743

[30] C. Hernández, F. Rodríguez, J. C. M. Moreno, P. R. da Costa Mendes, and J. E. Normey-Rico, "An optimal approach to microgrid power distribution using Model-based Predictive Control (MPC): a case study simulation," *Actas de las XXXVII Jornadas de Automática 7, 8 y 9 de septiembre de 2016, Madrid*, 2022, [Online]. Available: https://api.semanticscholar.org/CorpusID:247100068